Potential benefits of dihydroartemisinin in suppression of dexamethasone induced osteoporosis, osteoclast formation and RANKL induced signaling pathways in adult female albino rat

Omnia S. Erfan[1], Yassmin G. Salem[1], Mona A. El-Shahat[1], Walaa F. Awadin[2], Huda Eltahry[1], Mamdouh Eldesoqui[1]

[1] *Department of Anatomy and Embryology, Faculty of Medicine, Mansoura University, Egypt*

[2] *Department of Pathology, Faculty of Veterinary Medicine, Mansoura University, Egypt*

SUMMARY

Osteoporosis is a musculoskeletal disorder characterized by reduced bone density and increased susceptibility to fractures. Fractures cause a considerable increase in mortality, disability, and morbidity incidence. Artemisia annua is a medicinal plant, used for long time in Asian countries and its active metabolite is Dihydroartemisinin (DHA). It is proven to possess anti-inflammatory and antioxidant effects. The present study is the first to investigate the role of different doses of DHA in treatment of Dexamethasone (Dexa)-induced osteoporosis. Thirty female Wister adult rats were divided into three groups for three months. Control and Dexa groups were both six in number. Dihydroartemisinin treated groups, eighteen in number, received intramuscular injection of Dexamethasone and intraperitoneal injection of DHA, then subdivided in three different groups according to DHA doses (10, 20 and 30 mg/kg body wight). Blood level of Ca, P, calcitonin, alkaline and acid phosphatase, and Tissue MDA, GSH were estimated. Tibiae were stained with H&E, Masson-Goldner, and immunological examination of β catenin and RANKL was done. Then, one-way ANOVA test, followed by Tukey's post-hoc test, was used in order to compare groups, and P value <0.05 was considered statistically significant.

A highest dose of DHA showed normalization of blood parameter and oxidative stress markers. Also, bone histology improvement, reduced RANKL and increased β catenin expression were recorded. Treatment with DHA has significantly improved the oxidative stress, biochemical parameters, and bone histology. Dihydroartemisinin might represent a novel approach for modulation of osteoporosis induced by glucocorticoid.

Key words: Dihydroartemisinin – RANKL – Osteoporosis – Dexamethasone – β-catenin

Corresponding author:
Omnia Sameer Erfan. Department of Anatomy and Embryology, Faculty of Medicine, Mansoura University, Egypt. Phone: 00201552523630. E-mail: Omnia.sameer@gmail.com

Submitted: February 4, 2022. **Accepted:** May 3, 2022

https://doi.org/10.52083/ITUY9072

INTRODUCTION

Osteoporosis is a musculoskeletal disorder characterized by reduced bone density and enhanced susceptibility to fractures. Osteoporosis is a silent disease without any apparent symptoms till a fracture occurs (Sozen and Ozer, 2017). These fractures lead to significant mortality and morbidity and result in socio-economic costs, including direct medical and indirect expenses resulting from decreased quality of life and disabilities (Willson et al., 2015).

Osteopetrosis results from the disturbance in the balance between bone formation by osteoblasts and bone resorption by osteoclasts (Ahmadzadeh et al., 2016). Osteoclast formation and activation is primarily regulated by the receptor activator of nuclear factor kappa-B ligand (RANKL). The interaction between RANKL and its receptor RANK activates several transcription factors that in turn activate the expression of genes regulating osteoclast differentiation and function (Zhou et al., 2016). Proliferation and differentiation of osteoblastic precursors, and maintenance of mature osteoblasts ar regulated by the Wnt/β-catenin pathway (Baron et al., 2006).

Glucocorticoids represent the first option used during treatment of various chronic and autoimmune diseases, and in organ transplantation (Fang et al., 2021). Osteoporosis is one of the major sequels following treatment with glucocorticoid (GC), known as secondary osteoporosis (Hartmann et al., 2016). Glucocorticoid therapy suppresses osteoblast function and bone formation; on the other hand, it boosts bone resorption, reduces calcium absorption and inhibits endogenous gonadal steroids, all of which lead to enhanced bone loss (Ioannidis et al., 2014).

Appropriate nutrition, weight bearing exercise, calcium, vitamin D supplements, and pharmacological therapies could minimize bone loss (Gallagher and Sai, 2010). Lee et al. (2017) reported that long-term use of pharmacological therapies possesses different adverse effects, such as bisphosphonates (osteonecrosis of the jaw and nephrotoxicity), estrogen replacement therapy, (risk of cardiovascular disease and breast cancer), teriparatide, (temporary rises in serum and urine calcium levels), and denosumab, (reduce serum calcium level).

Artemisia annua is a medicinal plant, which has been used for a long time to treat different diseases in Asian countries (Katiyar et al., 2012). It has been used safely for treatment of malaria, as it acts by killing plasmodium parasites through induction of iron-dependent oxidative stress (Cabello et al., 2012). Many studies used Artemisia annua extract and its active compound artemisinin to develop more effective drug against malaria (Chaturvedi et al., 2010). Artemisinins have proven to have anti-inflammatory, antioxidant, anti-cancer and anti-microbial activities (Ferreira et al., 2010). Dihydroartemisinin (DHA) is known to be the active ingredient of the artemisinin compounds. The present experiment aimed to investigate the role of DHA in the management of Dexamethasone (Dexa)-induced osteoporosis.

MATERIALS AND METHODS

Experimental animals

Thirty adult female Wister albino rats (12-14 weeks old) weighting 200-250 g were used in this study. Rats were kept under controlled condition of temperature (23±3 °C), and relative humidity throughout the whole study period, with stable 12/12-hours light/dark cycle. Three animals were housed per cage, with free access to water and *ad libitum* diet. The housing of the rats was conducted in the Faculty of Medicine, Mansoura University. The experiment was conducted in accordance with the Animals' Experimentation Committee at Mansoura University and was authorized by Mansoura Faculty of Medicine, Institutional Research Board under the number of (MDP. 18.12.15.R1.R2). Significant efforts were made to minimize the number of animals used.

Experimental design and treatments

Rats were randomly allocated into three groups: Control group (n = 6): injected intraperitoneal with saline every 2 days; Dexamethasone (Dexa)-treated group (n=6): injected intramuscularly by Dexamethasone with dose of 1 mg/kg/BWT every 3 days (Liu et al., 2011); Dihydroartemisinin-treated

(D+D) groups (n=18): injected intramuscularly by Dexamethasone (1 mg/kg / BWT every 3 days), as well as intraperitoneal injection of dihydroartemisinin dissolved in saline every 2 days. They were divided into three subgroups according to the dose of dihydroartemisinin: D+D10 group (n = 6) received 10 mg/kg (Zhou et al., 2016), D+D20 group (n = 6) received 20 mg/kg, and D+D30 group (n = 6) received 30 mg/kg (Ge et al., 2018). The experiments lasted for three months.

Body weight measurement

At the end of the experiment, the weight of each animal was recorded with a digital electrical balance.

Blood collection

After three months, a retro-orbital blood sample was withdrawn from all animals, then centrifuged to separate serum. The serum was used to measure calcium, phosphorus, calcitonin, alkaline phosphatase, and acid phosphatase levels.

Bone specimen

The animals were anaesthetized deeply by intraperitoneal ketamine (90 mg/kg) and xylazine (15 mg/kg) just before scarification. From each animal, right tibiae were dissected out and cleaned from muscle and soft tissues. Also, left tibiae were dissected out from each animal then homogenized for quantitative analysis of oxidative stress markers (Sözen et al., 2017).

Biochemical studies

Serum was separated by centrifugation at 4000 rpm for 15 minutes for use in the biochemical assay. The serum was stored at −20°C before analysis, using a Synchron cx5 autoanalyzer (Beckman, CA, USA). Concentrations of calcium (Ca), phosphorus (P), alkaline phosphatase and acid phosphatase in the serum were determined spectrophotometrically using specific diagnostic reagent kits (Biodiagnostic kits, Giza, Egypt) and an Olympus AU 2700 analyzer (Mishima, Japan) (Chen et al., 2019). Calcitonin (CT) was determined in serum using ELISA kits obtained from Life Span Bioscience, Inc. (LSBio).

Evaluation of oxidative stress

Malondialdehyde (MDA) and reduced glutathione (GSH) were assessed in Bone homogenate of left tibiae, using colorimetric method applying the suitable kits (Biodiagnostic kits, Giza, Egypt) (El Wakf et al., 2014).

Histological and immunohistochemical stains

From each animal in each group, the collected tibiae were fixed for 4 days using 10% buffered formal saline, then decalcified with Ethylenediamine Tetra-acetic acid (EDTA) (Ge et al., 2018) for nearly 14 days, and then blocks of paraffin were prepared. Longitudinal sections of tibiae, with the thickness of 5 µm, were stained by hematoxylin and eosin (H&E) to evaluate bone histological changes, Masson Goldner to assess development of new bone, bone formation and resorption immunohistochemical marks (β-catenin and RANKL, respectively) supplied by New Test Company, Cairo, Egypt.

For immunohistochemical staining, sections on positively charged glass slides were de-paraffinized and rehydrated. Then sections were washed with distilled water, blocked in 0.1% hydrogen peroxide, and then rinsed for three times with phosphate-buffered saline (PBS). Protein block was used (5 minutes) to block nonspecific background. Then sections were rinsed by distilled water after that, and they were washed in PBS for three times. The different primary antibodies were incubated with slides overnight at 4° C. The used primary antibodies were rabbit polyclonal anti-RANKL (DF7006, Affinity Bioscience, USA, at 1/200 dilution) and rabbit monoclonal anti-Beta catenin antibody (IGX4794R-3, Gene Tex International Corporation, USA at 1/100 dilution). Following washing for three times by PBS for 5 minutes, the slides were incubated with biotinylated goat antipolyvent for 20 min. After that, slides were then incubated for 10 minutes together with conjugated streptavidin and rinsed out over again with PBS. Following that, slides were incubated with DAB substrate (diaminobenzidine) for 3 minutes (Mouse and

rabbit HRP/DAB (ABC) detection IHC kit, ab64264, Abcam, UK). Lastly, sections were counterstained using Mayer's hematoxylin for one minute.

Statistical analysis and measurements

Morphometric studies were done using Image J program (version 1.48, Wayne Rasband, National Institutes of Health, Bethesda, MD, USA), matching with the program instructions. Five sections of tibiae cut at different levels stained by H&E or immunostained were examined from five rats in every group. In H&E-stained slides, the bony trabeculae were assessed at their midpoint away from their branched areas. In every section, the mean trabecular thickness of five non-overlapping fields (at magnification x100) was estimated. The mean area percentage of immune positive reaction was calculated using five non overlapping fields (at magnification x400; area: 0.071 mm^2) for every RANKL and β-catenin stained- section (Shaalan et al., 2020).

Data were analyzed using computer program SPSS (Statistical Package for Social Science), version 22 (IBM, USA). Data were expressed as Mean ± Standard deviation. One-way ANOVA test, and then Tukey's post-hoc test were applied in order to compare different groups. The statistically significant rate was judged when P value below 0.05. All graphical data descriptions were performed with Microsoft Excel® for windows® (Microsoft Inc., USA).

RESULTS

Body weight

At the time of sacrifice, the body weight of Dexa group was highly significantly decreased compared to that of control group, and only the highest dose of DHA (D+D30) normalized the body weight, while both D+D10- and D+D20-treated groups showed a highly significant increase as compared to Dexa group (Fig. 1A).

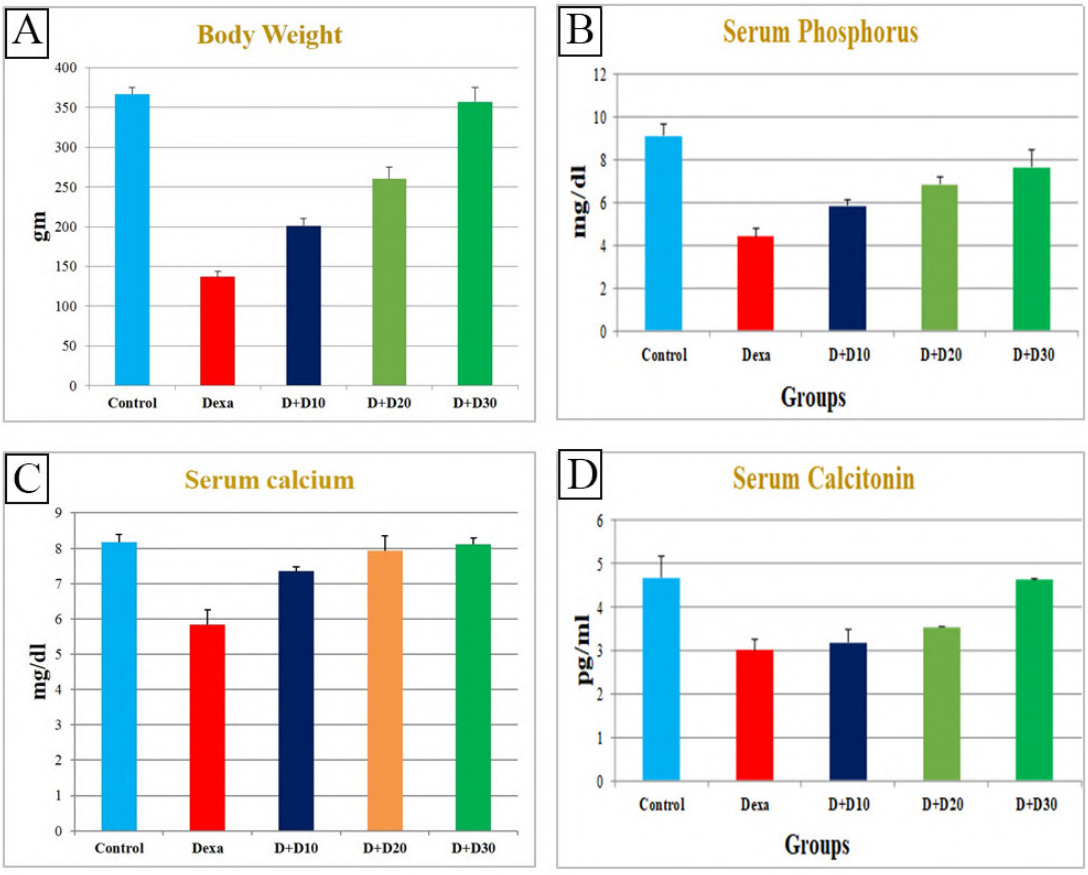

Fig. 1.- Body weight at the time of sacrifice in different groups (**1A**), Serum level of phosphorus in different groups (**1B**), Serum level of calcium in different groups (**1C**) and Serum level of calcitonin in different groups (**1D**).

Biochemical tests

Serum level of P in Dexa group was highly significantly decreased compared to that of control group, and all three doses of DHA showed a high significant increased compared to Dexa group (Fig. 1B). Serum level of Ca of the Dexa group was highly significantly decreased compared to that of control group. While compared to control, both doses of DHA 20 and 30 normalized the serum level of Ca, while the lower dose (D+D10) showed a high significant increase compared to Dexa-treated group (Fig. 1C).

Serum level of calcitonin of Dexa group was highly significantly decreased compared to that of control group, and only the high dose (D+D30) normalized serum level of calcitonin, while both D+D10- and D+D20-treated groups showed highly significant increased compared to Dexa group (Fig. 1D).

Serum level of alkaline and acid phosphatase of Dexa group was highly significantly increased compared to that of control group. Only the highest dose of DHA normalized serum both levels of alkaline and acid phosphatase while both D+D10 and D+D20 groups significantly decreased compared to that of Dexa group (Figs. 2C, 2D).

Oxidative stress markers

Bone tissue level of GSH in Dexa group was highly significantly decreased in comparison to the control group. Compared with control rats, only the high dose (D+D30) normalized the GSH level, although in both D+D10 and D+D20 groups this was increased highly significantly compared to Dexa group (Fig. 2A).

Bone tissue level of MDA of Dexa group was highly significantly increased compared to that of the control group. Only the highest dose normalized the bone tissue level of MDA, althoughin both D+D10 and D+D20 groups this was highly significantly decreased compared to that of Dexa group (Fig. 2B).

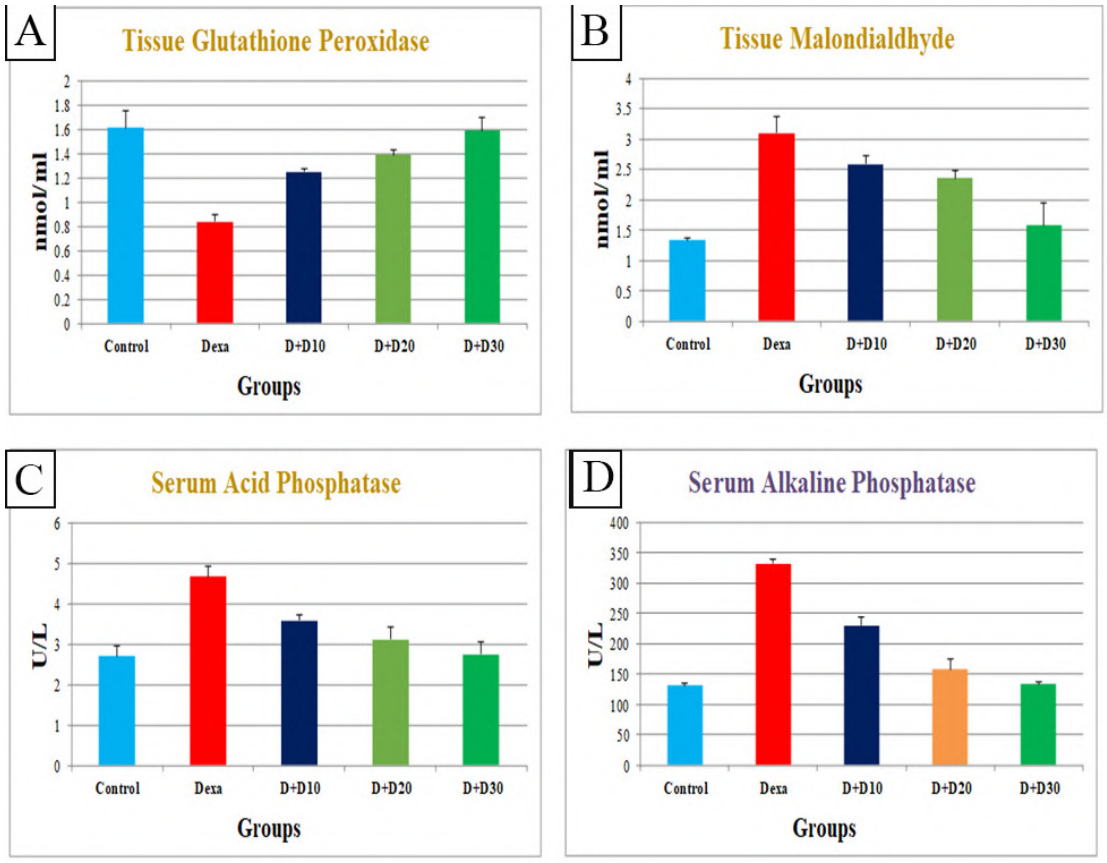

Fig. 2.- Bone tissue level of glutathione peroxidase in different groups (**2A**), Bone tissue level of MDA in different groups (**2B**), Serum level of acid phosphatase in different groups (**2C**) and Serum level of alkaline phosphatase in different groups (**2D**).

Histological Examination

Hematoxylin and Eosin-stained sections

The epiphysis of the tibia in the control group showed cancellous bone formed of bony trabecular networks separated by interconnecting spaces containing bone marrow formed of hemopoietic tissue, scattered adipocytes and seeming normal numbers of osteoclasts (Fig. 3A). Epiphysis of Dexa group showed apparent increase of the adipocytes in bone marrow as compared with control rats, with clear trabecular bone resorption indicated by widely separated thin bone spicules. Increased numbers of bone marrow adipocytes and osteoclasts were also observed (Fig. 3B). The effect of Dexa gradually reversed in DHA-treated groups with increasing dose from 10 to 30, as shown in gradual increase of the trabecular thickness, reduction of adipocytes and osteoclasts numbers contrasted to the Dexa-treated rats (Figs. 3C, D and E). Statically, the trabecular bone thickness in the epiphysis of the Dexa group was significantly decreased compared to that of the control group. Trabecular bone thickness in the epiphysis of D+D30-treated group was highly significantly increased compared to that of Dexa group and both groups (D+D10 and D+D20) showed a significant increase compared to that of Dexa group. Moreover, the three doses of DHA normalized the trabecular bone thickness (Fig. 3F).

The diaphysis of control group sections showed compact bone covered from outside by regular periosteum, and from inside by smooth endosteal surface (Fig. 4A). Osteocytes inside their lacunae and osteoblasts on bone surface and regularly arranged collagen fibers were seen. the diaphysis from the Dexa group (Fig. 4B) showed irregularly eroded endosteal surface. Empty lacunae, osteoclast housed in the eroded area in bone surface with faintly stained matrix were observed. the diaphysis from the D+D10 group showed compact bone with regular periosteum and endosteum with some empty lacunae. Higher magnification showed regularly arranged collagen fibers and some osteocytes inside their lacunae (Fig. 4C). The diaphysis from D+D20 and D+D30 groups showed compact bone with regular periosteum and endosteum (Fig. 4D, E).

Masson Goldner-stained sections

Masson Goldner-stained sections of tibia diaphysis (Fig. 5A) in the control group showed compact bone and tibia epiphysis (Fig. 6A), cancellous bone with regular appearance of mature bone, which is stained green, and average amount of red stained newly formed bone (Fig. 5A). In the Dexa group, a significant decline in red-stained newly formed bone was noticed (Figs. 5, 6B). The consequence of Dexa gradually inverted in treated groups, D+D corresponding to increasing dose from 10 to 30 mg, with noticeable rise of the red-stained newly formed bone in comparison to the Dexa treated rats (Figs. 5, 6C, D and E).

Immunostained sections

RANKL-stained sections

RANKL expression was nonexistent almost in bone marrow of control rats (Fig. 7A). Highly significant potent RANKL expression was observed in bone marrow of the Dexa-treated rats compared to that of the control group (Figs. 7B, F). Expression of RANKL in bone marrow significantly diminished with all DHA doses, D+D10 (Figs. 7C and F), D+D20 (Figs. 7D and F), and D+D30 (Figs. 7E and F), and both doses D+D20 and D+D30 restored the normal RANKL expression (Figs. 7C, D, E and F).

β *catenin-stained sections*

β-catenin expression was identified in the bone marrow of control rats (Fig. 8A). In Dexa-treated animals, β-catenin expression was not detected in bone marrow, with a significant high ($P< 0.001$) reduction in area percentage in comparison with control sections (Fig. 8B and F). β-catenin expression gradually raised in bone marrows of groups treated with D+D10, D+D20, and D+D30 when compared with the Dexa group. Also, it significantly ($P<0.001$) enhanced in comparison to the Dexa rats in both D+D20, and D+D30, but was non-significantly increased in D+D10 group (Figs. 8C, D, E and F).

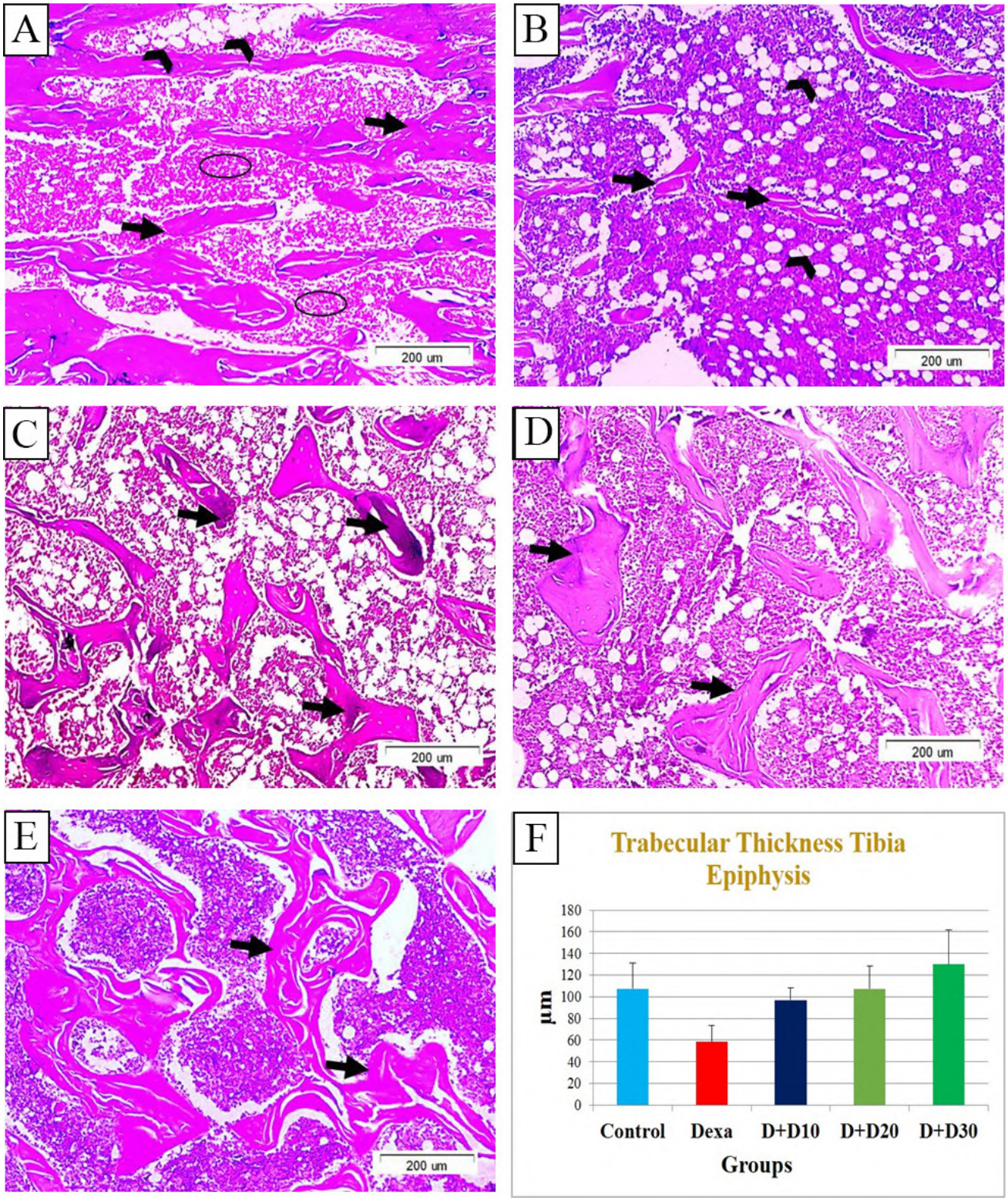

Fig. 3.- Tibia section from epiphysis stained with H&E the control group (**3A**) displaying cancellous bone arranged as networks of bony trabeculae (black arrows) separated by bone marrow interconnecting spaces made by hemopoietic tissue (circles) and dispersed adipocytes (arrowheads). The Dexa group (**3B**) showing apparent increase in the bone marrow adipocytes (arrowheads) compared to control sections. Significant trabecular bone resorption is seen and revealed as widely separated thin bone spicules (black arrows). The D+D10 group (**3C**) showing a slight increase in trabecular thickness (black arrows) as compared to Dexa group. The group treated with D+D20 (**3D**) showed an increase in trabecular thickness (black arrows) as compared to Dexa group and D+D10-treated group. The group treated with D+D30 (**3E**) showed a marked increase in trabecular thickness (black arrows) as compared to Dexa group and D+D10-treated groups, with well-developed thickened trabeculae when compared with the co group. (H&E, x100, scale bar = 200 µm). Trabecular bone thickness in the epiphysis of different groups (**3F**).

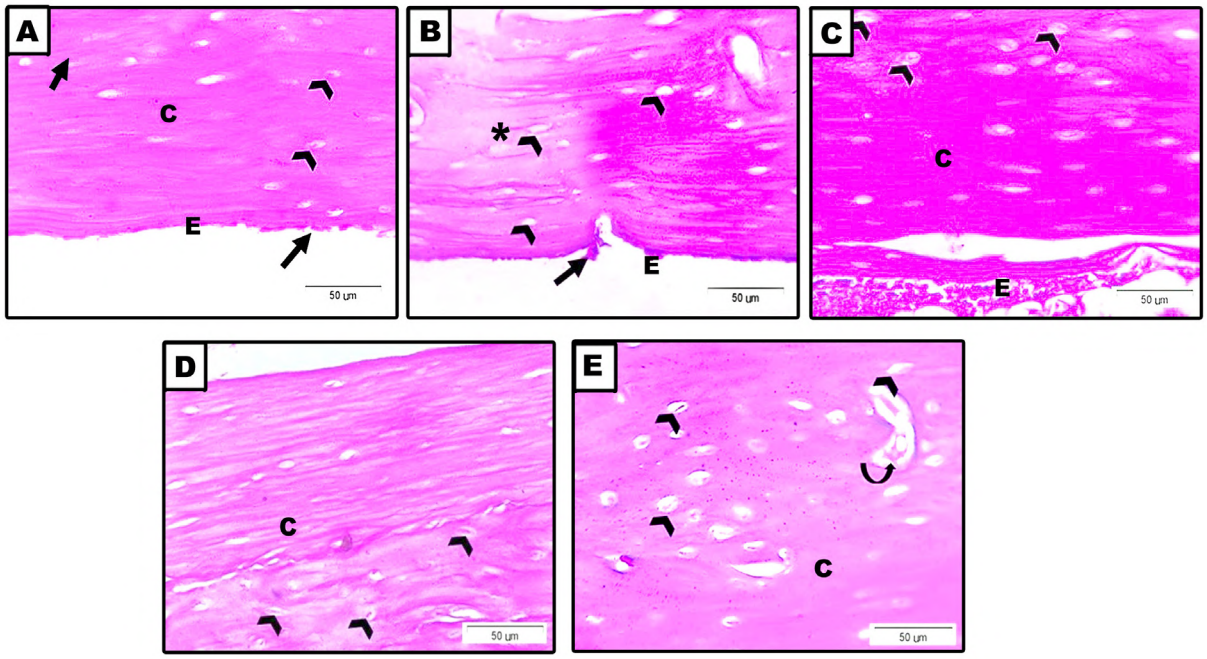

Fig. 4.- Tibia section from diaphysis of control group (**4A**) stained with H&E showing osteocytes inside their lacunae (arrowheads), smooth endosteal surface (E) lined with osteoblasts (black arrow) and regularly arranged collagen fibers (C). Dexa group (**4B**) showing empty lacunae (arrowheads), osteoclast housed in the eroded area in bone surface (black arrows) with faintly stained matrix (*) irregularly and eroded endosteal surface (E). D+D10 (**4C**) stained with H&E showing compact bone with regular arrangement of collagenous fibers of matrix (C) and osteocytes inside their lacunae (arrowheads). D+D20 (**4D**) stained with H&E showing compact bone with regularly arranged collagenous fibers of matrix (C) and osteocytes inside their lacunae (arrowheads). D+D30 (**4E**) group stained with H&E showing compact bone with regularly arranged collagenous fibers of matrix (C) and osteocytes within their lacunae (arrowheads). Blood vessel (curved arrow) is seen. (H&E, x400, scale bar = 50 µm).

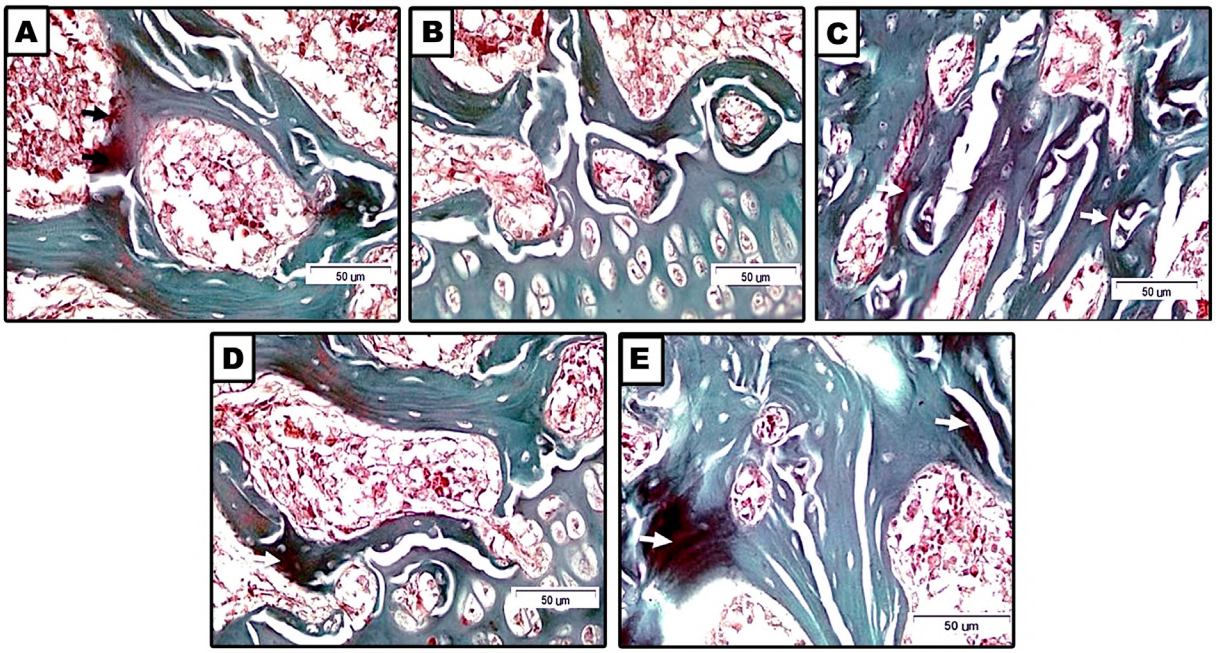

Fig. 5.- Masson Goldner-stained tibia section of the epiphysis of control group (**5A**) showing typical green stained mature compact bone look and average amount of red stained newly formed bone. The epiphysis of Dexa group (**5B**) showing significant decrease of red stained newly constructed bone. The epiphysis of D+D10 group (**5C**) showing enhanced red stained newly formed bone in comparison with Dexa-treated rats. The epiphysis of D+D20 group (**5D**) showing increased red stained newly formed bone as compared to Dexa-treated rats. Epiphysis of D+D30 group (**5E**) showing markedly enhanced red stained newly formed bone (white arrows) in comparison to Dexa section. (Masson Goldner, x400, scale bar = 50 µm).

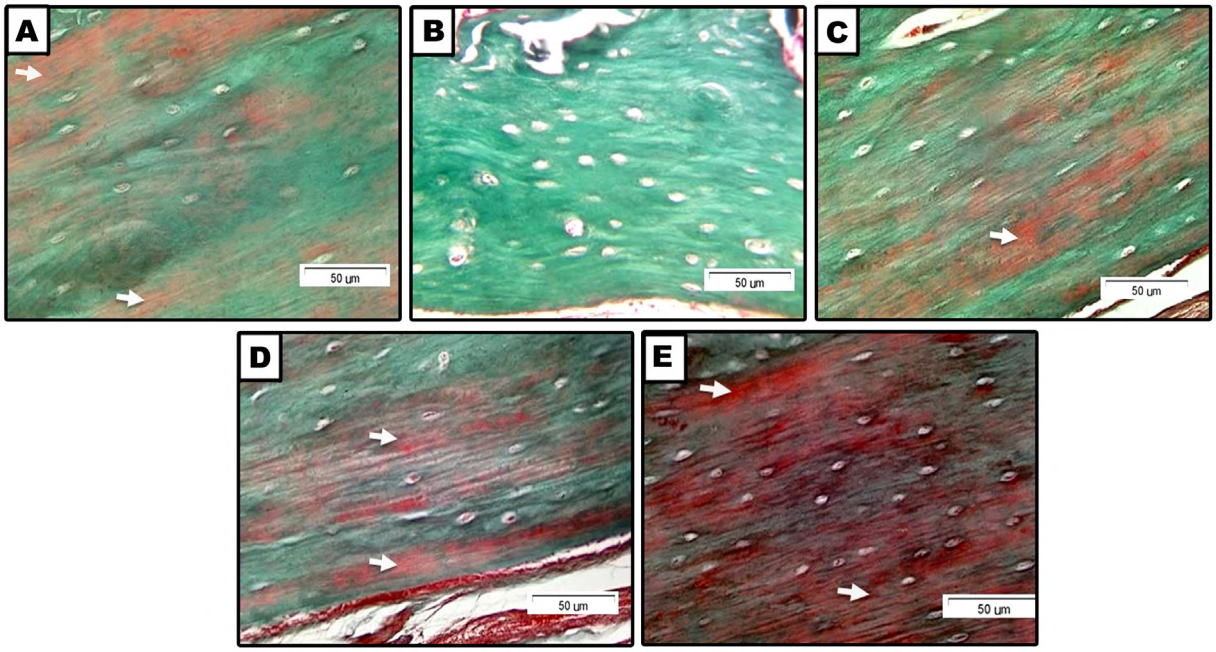

Fig. 6.- Masson Goldner stained of tibia diaphysis control group (**6A**) showing typical look of green colored mature compact bone with average amount of newly formed bone which is stained red. Dexa group (**6B**) showing noticeable decrease of red colored newly formed bone. D+D10 group (**6C**) showing enhanced red colored newly formed bone in comparison to Dexa sections. D+D20 rats (**6D**) showing elevated amount of red colored newly formed bone when compared to Dexa-treated rats. D+D30 group (**6E**) showing significantly enhanced red colored newly formed bone when compared to Dexa treated animals (Masson Goldner, x400, scale bar = 50 µm).

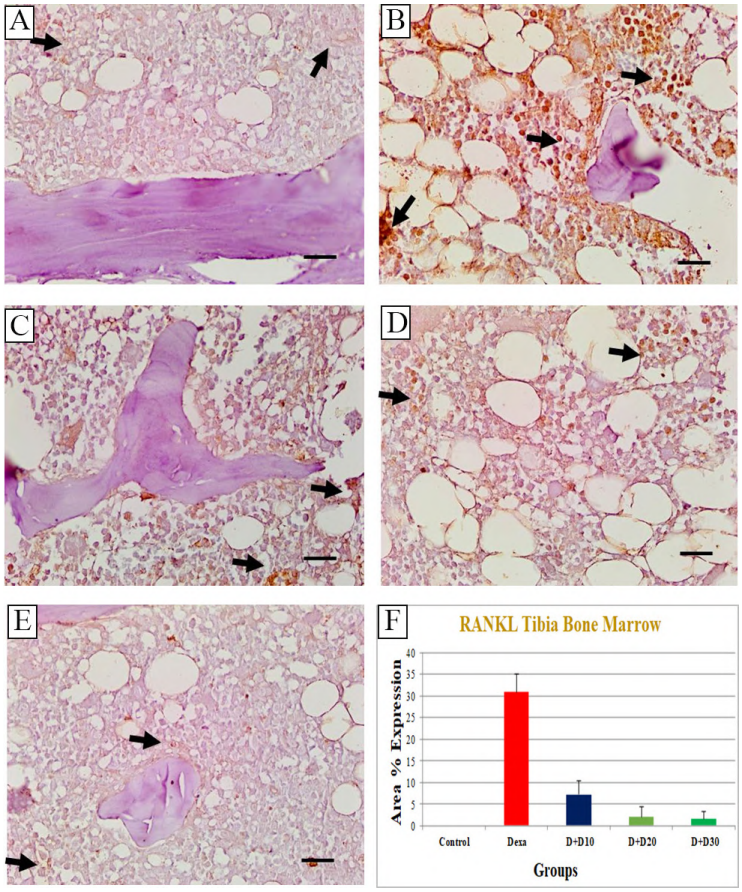

Fig. 7.- Tibia section immunostained against RANKL control group (**7A**) showing weak RANKL expression (black arrows) in bone marrow. Dexa group (**7B**) showing strong expression (black arrows) against RANKL in the bone marrow. D+D10 group (**7C**) showing moderate RANKL expression (black arrows) against as compared to Dexa group. D+D20 group (**7D**) showing mild expression (black arrows) against RANKL as compared to Dexa group. D+D30 group (**7E**) showing mild expression (black arrows) against RANKL in the bone marrow as compared to Dexa group. (RANKL immunohistochemistry, x400, bar = 50 µm). RANKL expression by area % in Dexa group (**7F**).

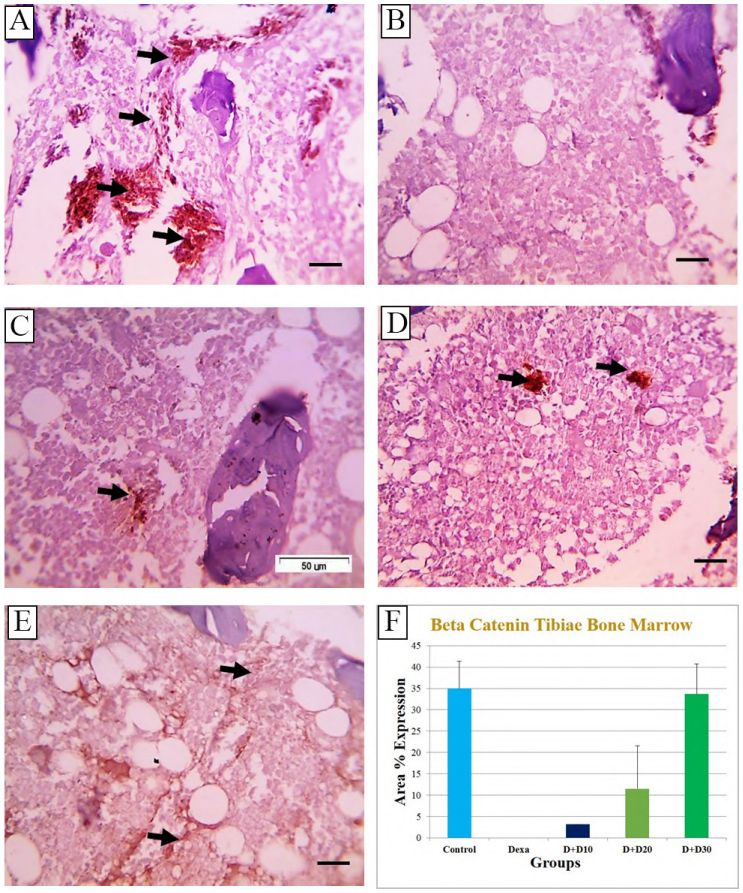

Fig. 8.- Tibia section immunostained against β catenin, control group (**8A**) showing strong β catenin expression in the bone marrow. Dexa-treated rats (**8B**) showing nearly absent expression in the bone marrow. D+D10 group (**8C**) showing mild increase of β catenin expression (black arrow) in the bone marrow as compared with Dexa group. D+D20 group (**8D**) showing moderate increase of β catenin expression (black arrow) in the bone marrow as compared with Dexa group. D+D30 group (**8E**) showing marked increase of β catenin expression (black arrows) in the bone marrow as compared with Dexa group. (β catenin immunohistochemistry, x400, scale bar = 50 µm). β catenin expression by area % in different groups (**8F**).

DISCUSSION

In this study, we used the glucocorticoid osteoporotic rat model to elucidate the protective effect of the antimalarial active compound in Artemisia Annua plant, the artemisinin against the development of osteoporosis. Glucocorticoids (GCs) induce osteoporosis via multiple mechanisms; they decrease bone formation, suppress the production of bone matrix, enhance apoptosis of the osteoblasts (Gohel et al., 1999) and increase resorption of bone by increase the numbers of the osteoclasts (Frenkel et al., 2015). Corticosteroids-induced oxidative stress provoke apoptosis, osteonecrosis and osteoporosis (Kerachian et al., 2006). Reactive oxygen species (ROS) can induce necrosis or apoptosis through Bcl-2 family proteins, mitochondrial dysfunction, and caspase stimulation. In addition, ROS can promote osteoclast differentiation (Callaway et al., 2015).

Corticosteroids induce bone resorption through the expression of receptor activator RANKL cytokine, which is necessary for osteoclast development. On the other hand, GCs downregulate the osteoprotegerin receptor (OPG) that blocks RANKL binding to RANK (Sivagurunathan et al., 2005). Kondo et al. (2008) reported that Osteoprotegerin impedes osteoclast differentiation, survival, and function in vitro and bone resorption in vivo. The imbalance between RANKL and OPG eventually results in a state of increased osteoclastogenesis and accelerated the rate of bone resorption (Boyce and Xing, 2008).

Osteoblasts and adipocytes originate from common mesenchymal progenitors (Prockop, 1997). The GCs inhibit bone formation through suppression of osteoblast proliferation, and it directs the mesenchymal progenitor cells in the direction of adipocyte lineage (Canalis

et al., 2007). The Wnt/ß-catenin signaling is the determining factor of the cell fate of pre-osteoblasts (Song et al., 2012). Activation of Wnt/ß-catenin stimulates the differentiation of osteoblasts, enhances the osteoblastogenesis and prevents their apoptosis (Duan and Bonewald, 2016). On the other hand, activation of Wnt/ß-catenin signaling inhibits adipogenesis from the mesenchymal precursors (Krishnan et al., 2006). Wnt/ß-catenin signals in osteoblasts induce OPG expression and thereby suppress the osteoclast differentiation (Kondo et al., 2008). Naito et al. (2012) reported that Corticosteroids can suppress Wnt/b-catenin activity via activation of GSK3b and downregulating ß-catenin. In addition, GCs induced RANKL signalling also increase degradation and inhibit synthesis of ß-catenin (Chen et al., 2018).

Many studies have demonstrated that Artemisia-annua-derived compounds, artemisinins (ARS), protects from bone loss in several animal models of induced bone loss. As in mouse model of different diseases, ovariectomized mice (Lee et al., 2017), lipopolysaccharide (LPS)-induced bone loss model (Wei et al., 2018), titanium-particle induced osteolysis (Feng et al., 2016), and in rat model of inflammatory bowel disease-related bone loss (Ge et al., 2018).

Up to our knowledge, this is the first study which use dihydroartemisinin (DHA) in treatment of Dexa-induced osteoporosis, and it showed increasing effects with dose increment as proven histological, immunohistochemical and biochemical tests. Also, thickness of bony trabeculae increased with new bone formation and in the bone marrow, expression of RANKL decreased while β-catenin was raised. The serum levels of Ca, P and calcitonin increased while alkaline phosphatase and acid phosphatase decreased. In bony tissue homogenate, the lipid peroxidation was reduced as indicated by the decrease of MDA, and the oxidative stress state decreased as was evident by the elevation of GSH.

The antioxidant effects of Artemisia annua is believed to be related to its flavonoids contents, which are capable of neutralizing free radicals present in the cell environment, and prevent their damaging effects (Lang et al., 2019). Flavonoids likewise prevent lipid peroxidation and increase the activity of antioxidant system (Kim et al., 2003). Artemisia plant extract also hinders activity of heme oxygenase, therefore reducing free radicals creation (Jafari Dinani et al., 2007).

In the current study, DHA markedly inhibited the expression of receptor activator of nuclear factor-κB ligand (RANKL) in the bone marrow. Thus, RANKL-stimulated osteoclast differentiation in bone-marrow-derived macrophages is supressed by diminished osteoclastogenesis and suppressed bone resorption. These repressing effects might be facilitated by inhibitions of multiple signalling pathways such as decreased expression of c-Fos and nuclear factor of activated T-cells (NFATc1) (Lee et al., 2017), nuclear factor kappa-B (NF-κB) (Wei et al., 2018), mitogen-activated protein kinases (MAPKs) (Wu et al., 2018), phospholipase Cγ1 (PLCγ1)-Ca2+-NFATc1 (Zeng et al., 2017), and protein kinase B (PKB/AKT)/SRC (Feng et al., 2016). Lee et al. (2017) suggested that Artemisia annua extract may reduce bone loss through inhibiting RANKL-induced osteoclast differentiation, instead of controlling RANKL and/or OPG production in proinflammatory cytokine-stimulated osteoblastic cells.

In a mouse model of lipopolysaccharide (LPS)-induced bone loss, artesunate suppressed osteoclastogenesis and bone resorption. However, it did not affect osteoblast mediated bone formation (Wei et al., 2018). In particular, ARS compounds might induce oxidative damage in osteoclasts that have higher intracellular iron level than other cells (Zhang, 2020). Intracellular iron may trigger ARS compounds, causing release of huge amount of free radical (Chaturvedi et al., 2010). Any reason able to increases ROS may lead to oxidative damage to osteoclasts which already have increased level of ROS (Domazetovic et al., 2017). Accumulation of ROS increases cytochrome c and AIF release from mitochondria to the cytosol, with the stimulation of caspase-3 and rise of the Bax/Bcl-2 ratio (Dou et al., 2016).

However, Fang et al. (2021) demonstrated that artemisinin treatment increased survival of bone marrow mesenchymal stromal cells by suppression of ROS production that associated with the reduction of caspase-3 activation, and

apoptosis induced by Dexa. This may be related to the decreased oxidative stress in bone-marrow mesenchymal cells prior to their differentiation into osteoclasts, which cause them to be less vulnerable to DHA-stimulated apoptosis (Dou et al., 2016).

Moreover, in this research, DHA improved the expression of β-catenin in bone marrow, which may indicate stimulation of osteoblastogenesis. This was manifested by new formations in both the trabecular and cancellous bone as detected by Masson Goldner stain. (Nemeth et al., 2009). Tay et al. (2017) showed that ß-catenin deficient bone marrow exhibited decreased numbers of osteoblasts in vitro and in vivo, with diminished production of the hematopoietic regulatory factors; basic fibroblast growth factor (bFGF), SCF, and VCAM-1. ß-catenin is essential for production of osteoblasts and the preservation of hematopoietic progenitors in the adult bone marrow (Nemeth et al., 2009). The Wnt canonical pathway regulates the proliferation and differentiation of osteoblastic precursors and retains mature osteoblasts (Baron et al., 2006).

In conclusion, this study showed that treatment with DHA to Dexa-induced model of osteoporosis significantly improved the oxidative stress, biochemical and histological bone indices. It exerted its effects through stimulation of the Wnt-β catenin and inhibition of RANKL pathways, which is reflected on stimulation of osteoblastogenesis and inhibition of osteoclastogenesis. Dihydroartemisinin may be a new treatment approach to avoid glucocorticoid-induced osteoporosis.

REFERENCES

AHMADZADEH A, NOROZI F, SHAHRABI S, SHAHJAHANI M, SAKI N (2016) Wnt/β-catenin signaling in bone marrow niche. *Cell Tissue Res,* 363(2): 321-335.

BARON R, RAWADI G, ROMAN-ROMAN S (2006) Wnt signaling: a key regulator of bone mass. *Curr Top Dev Biol,* 76: 103-127.

BOYCE BF, XING L (2008) Functions of RANKL/RANK/OPG in bone modeling and remodeling. *Arch Biochem Biophys,* 473(2): 139-146.

CABELLO CM, LAMORE SD, BAIR WB 3RD, QIAO S, AZIMIAN S, LESSON JL, WONDRAK GT (2012) The redox antimalarial dihydroartemisinin targets human metastatic melanoma cells but not primary melanocytes with induction of NOXA-dependent apoptosis. *Invest New Drugs,* 30(4): 1289-1301.

CALLAWAY DA, JIANG JX (2015) Reactive oxygen species and oxidative stress in osteoclastogenesis, skeletal aging and bone diseases. *J Bone Miner Metab,* 33(4): 359-370.

CANALIS E, MAZZIOTTI G, GIUSTINA A, BILEZIKIAN JP (2007) Glucocorticoid-induced osteoporosis: pathophysiology and therapy. *Osteoporos Int,* 18(10): 1319-1328.

CHATURVEDI D, GOSWAMI A, SAIKIA PP, BARUA NC, RAO PG (2010) Artemisinin and its derivatives: a novel class of anti-malarial and anti-cancer agents. *Chem Soc Rev,* 39(2): 435-454.

CHEN C, ZHENG H, QI S (2019) Genistein and silicon synergistically protects against ovariectomy-induced bone loss through upregulating OPG/RANKL ratio. *Biol Trace Elem Res,* 188(2): 441-450.

CHEN X, ZHI X, WANG J, SU J (2018) RANKL signaling in bone marrow mesenchymal stem cells negatively regulates osteoblastic bone formation. *Bone Res,* 27(6): 34.

DOMAZETOVIC V, MARCUCCI G, IANTOMASI T, BRANDI ML, VINCENZINI MT (2017) Oxidative stress in bone remodeling: role of antioxidants. *Clin Cases Miner Bone Metab,* 14(2): 209-216.

DOU C, DING N, XING J, ZHAO C, KANG F, HOU T, QUAN H, CHEN Y, DAI Q, LUO F, XU J, DONG S (2016) Dihydroartemisinin attenuates lipopolysaccharide-induced osteoclastogenesis and bone loss via the mitochondria-dependent apoptosis pathway. *Cell Death Dis,* 7(3): e2162.

DUAN P, BONEWALD LF (2016) The role of the wnt/β-catenin signaling pathway in formation and maintenance of bone and teeth. *Int J Biochem Cell Biol,* 77(Pt A): 23-29.

EL WAKF AM, HASSAN HA, GHARIB NS (2014) Osteoprotective effect of soybean and sesame oils in ovariectomized rats via estrogen-like mechanism. *Cytotechnology,* 66(2): 335-343.

FANG J, SILVA M, LIN R, ZHOU W, CHEN Y, ZHENG W (2021) Artemisinin reverses glucocorticoid-induced injury in bone marrow-derived mesenchymal stem cells through regulation of ERK1/2-CREB signaling pathway. *Oxid Med Cell Longev,* 2021: 5574932.

FENG MX, HONG JX, WANG Q, FAN YY, YUAN CT, LEI XH, ZHU M, QIN A, CHEN HX, HONG D (2016) Dihydroartemisinin prevents breast cancer-induced osteolysis via inhibiting both breast caner cells and osteoclasts. *Sci Rep,* 6: 19074.

FERREIRA JF, LUTHRIA DL, SASAKI T, HEYERICK A (2010) Flavonoids from Artemisia annua L. as antioxidants and their potential synergism with artemisinin against malaria and cancer. *Molecules,* 15(5): 3135-3170.

FRENKEL B, WHITE W, TUCKERMANN J (2015) Glucocorticoid-induced osteoporosis. *Adv Exp Med Biol,* 872: 179-215.

GALLAGHER JC, SAI AJ (2010) Molecular biology of bone remodeling: implications for new therapeutic targets for osteoporosis. *Maturitas.* 65(4): 301-307.

GE X, CHEN Z, XU Z, LV F, ZHANG K, YANG Y (2018) The effects of dihydroartemisinin on inflammatory bowel disease-related bone loss in a rat model. *Exp Biol Med (Maywood),* 243(8): 715-724.

GOHEL A, MCCARTHY MB, GRONOWICZ G (1999) Estrogen prevents glucocorticoid-induced apoptosis in osteoblasts in vivo and in vitro. *Endocrinology,* 140(11): 5339-5347.

HARTMANN K, KOENEN M, SCHAUER S, WITTIG-BLAICH S, AHMAD M, BASCHANT U, TUCKERMANN JP (2016) Molecular actions of glucocorticoids in cartilage and bone during health, disease, and steroid therapy. *Physiol Rev,* 96(2): 409-447.

IOANNIDIS G, PALLAN S, PAPAIOANNOU A, MULGUND M, RIOS L, MA J, THABANE L, DAVISON KS, JOSSE RG, KOVACS CS, KREIGER N, OLSZYNSKI WP, PRIOR JC, TOWHEED T, ADACHI JD; CAMOS RESEARCH GROUP (2014) Glucocorticoids predict 10-year fragility fracture risk in a population-based ambulatory cohort of men and women: Canadian Multicentre Osteoporosis Study (CaMos). *Arch Osteoporos,* 9: 169.

JAFARI DINANI N, ASGARY S, MADANI H, MAHZONI P, NADERI G (2007) Effect of *Artemisia aucheri e*xtract on atherogenic lipids and atherogenesis in hypercholesterolemic rabbits. *J Med Plants,* 6(23): 20-28.

KATIYAR C, GUPTA A, KANJILAL S, KATIYAR S (2012) Drug discovery from plant sources: An integrated approach. *Ayu,* 33(1): 10-19.

KERACHIAN MA, HARVEY EJ, COURNOYER D, CHOW TY, SÉGUIN C (2006) Avascular necrosis of the femoral head: vascular hypotheses. *Endothelium,* 13(4): 237-244.

KIM KS, LEE S, LEE YS, JUNG SH, PARK Y, SHIN KH, KIM BK (2003) Anti-oxidant activities of the extracts from the herbs of Artemisia apiacea. *J Ethnopharmacol,* 85(1): 69-72.

KONDO T, KITAZAWA R, YAMAGUCHI A, KITAZAWA S (2008) Dexamethasone promotes osteoclastogenesis by inhibiting osteoprotegerin through multiple levels. *J Cell Biochem,* 1;103(1): 335-345.

KRISHNAN V, BRYANT HU, MACDOUGALD OA (2006) Regulation of bone mass by Wnt signaling. *J Clin Invest,* 116(5): 1202-1209.

LANG SJ, SCHMIECH M, HAFNER S, PAETZ C, STEINBORN C, HUBER R, GAAFARY ME, WERNER K, SCHMIDT CQ, SYROVETS T, SIMMET T (2019) Antitumor activity of an Artemisia annua herbal preparation and identification of active ingredients. *Phytomedicine,* 62: 152962.

LEE SK, KIM H, PARK J, KIM HJ, KIM KR, SON SH, PARK KK, CHUNG WY (2017) Artemisia annua extract prevents ovariectomy-induced bone loss by blocking receptor activator of nuclear factor kappa-B ligand-induced differentiation of osteoclasts. *Sci Rep,* 7(1): 17332.

LIU Y, CHEN Y, ZHAO H, ZHONG L, WU L, CUI L (2011) Effects of different doses of dexamethasone on bone qualities in rats. S*heng Wu Yi Xue Gong Cheng Xue Za Zhi,* 28(4): 737-743.

NAITO M, OMOTEYAMA K, MIKAMI Y, TAKAHASHI T, TAKAGI M (2012) Inhibition of Wnt/β-catenin signaling by dexamethasone promotes adipocyte differentiation in mesenchymal progenitor cells, ROB-C26. *Histochem Cell Biol,* 138(6): 833-845.

NEMETH MJ, MAK KK, YANG Y, BODINE DM (2009) beta-Catenin expression in the bone marrow microenvironment is required for long-term maintenance of primitive hematopoietic cells. *Stem Cells,* 27(5): 1109-1119.

PROCKOP DJ (1997) Marrow stromal cells as stem cells for nonhematopoietic tissues. *Science,* 276(5309): 717-724.

SHAALAN AAM, EL-SHERBINY M, EL-ABASERI TB, SHOAEIR MZ, ABDEL-AZIZ TM, MOHAMED MI, ZAITONE SA, MOHAMMAD HMF (2020) Supplement with calcium or alendronate suppresses osteopenia due to long term rabeprazole treatment in female mice: influence on bone TRAP and osteopontin levels. *Front Pharmacol,* 13(11): 583.

SIVAGURUNATHAN S, MUIR MM, BRENNAN TC, SEALE JP, MASON RS (2005) Influence of glucocorticoids on human osteoclast generation and activity. *J Bone Miner Res,* 20(3): 390-398.

SONG L, LIU M, ONO N, BRINGHURST FR, KRONENBERG HM, GUO J (2012) Loss of wnt/β-catenin signaling causes cell fate shift of preosteoblasts from osteoblasts to adipocytes. *J Bone Miner Res,* 27(11): 2344-2358.

SOZEN E, OZER NK (2017) Impact of high cholesterol and endoplasmic reticulum stress on metabolic diseases: An updated mini-review. *Redox Biol,* 12: 456-461.

SÖZEN T, ÖZIŞIK L, BAŞARAN NÇ (2017) An overview and management of osteoporosis. *Eur J Rheumatol,* 4(1): 46-56.

TAY J, LEVESQUE JP, WINKLER IG (2017) Cellular players of hematopoietic stem cell mobilization in the bone marrow niche. *Int J Hematol,* 105(2): 129-140.

WEI CM, LIU Q, SONG FM, LIN XX, SU YJ, XU J, HUANG L, ZONG SH, ZHAO JM (2018) Artesunate inhibits RANKL-induced osteoclastogenesis and bone resorption in vitro and prevents LPS-induced bone loss in vivo. *J Cell Physiol,* 233(1): 476-485.

WILLSON T, NELSON SD, NEWBOLD J, NELSON RE, LAFLEUR J (2015) The clinical epidemiology of male osteoporosis: a review of the recent literature. *Clin Epidemiol,* 9(7): 65-76.

WU H, HU B, ZHOU X, ZHOU C, MENG J, YANG Y, ZHAO X, SHI Z, YAN S (2018) Artemether attenuates LPS-induced inflammatory bone loss by inhibiting osteoclastogenesis and bone resorption via suppression of MAPK signaling pathway. *Cell Death Dis,* 9(5): 498.

ZENG X, ZHANG Y, WANG S, WANG K, TAO L, ZOU M, CHEN N, XU J, LIU S, LI XJBP (2017) Artesunate suppresses RANKL-induced osteoclastogenesis through inhibition of PLCγ1-Ca2+–NFATc1 signaling pathway and prevents ovariectomy-induced bone loss. *Biochem Pharmacol,* 15(124): 57-68.

ZHANG J (2020) The osteoprotective effects of artemisinin compounds and the possible mechanisms associated with intracellular iron: A review of in vivo and in vitro studies. *Environ Toxicol Pharmacol,* 76: 103358.